On Larger H_0 Values in the CMB Dipole Direction

Orlando Luongo,[1,2,3,4,*] Marco Muccino,[3,4,5,†] Eoin Ó Colgáin,[6,7,‡] M. M. Sheikh-Jabbari,[8,§] and Lu Yin[6,7,¶]

[1]*Dipartimento di Matematica, Università di Pisa, Largo B. Pontecorvo 5, Pisa, 56127, Italy.*
[2]*Divisione di Fisica, Università di Camerino, Via Madonna delle Carceri, 9, 62032, Italy.*
[3]*Al-Farabi Kazakh National University, Al-Farabi av. 71, 050040 Almaty, Kazakhstan.*
[4]*National Nanotechnology Laboratory of Open Type, Almaty 050040, Kazakhstan.*
[5]*Istituto Nazionale di Fisica Nucleare (INFN), Laboratori Nazionali di Frascati, 00044 Frascati, Italy.*
[6]*Center for Quantum Spacetime, Sogang University, Seoul 121-742, Korea.*
[7]*Department of Physics, Sogang University, Seoul 121-742, Korea.*
[8]*School of Physics, Institute for Research in Fundamental Sciences (IPM), P.O.Box 19395-5531, Tehran, Iran.*

On the assumption that quasars (QSO) and gamma-ray bursts (GRB) represent *standardisable candles*, we provide evidence that the Hubble constant H_0 adopts larger values in hemispheres aligned with the CMB dipole direction. The observation is consistent with similar trends in strong lensing time delay, Type Ia supernovae (SN) and with well documented discrepancies in the cosmic dipole. Therefore, not only do strong lensing time delay, Type Ia SN, QSOs and GRBs seem to trace a consistent anisotropic Universe, but variations in H_0 across the sky suggest that Hubble tension is a symptom of a deeper cosmological malaise.

I. INTRODUCTION

Persistent cosmological tensions [1–7] suggest that it is timely to reflect on the success of the flat ΛCDM cosmology based on Planck values [8]. In particular, a $\sim 10\%$ discrepancy in the scale of the Hubble parameter in the post Planck era, *if true*, belies the moniker "precision cosmology". Recently, the community has gone to considerable efforts to address these discrepancies (see [9]), but proposals are often physically contrived. Great progress has been made in cosmology through the *assumption* that the Universe is isotropic and homogeneous, namely the Cosmological Principle or Friedmann-Lemaître-Robertson-Walker (FLRW) paradigm. Nevertheless, cosmological tensions point to something being amiss. Here, we present evidence that FLRW is suspect [10] (see [11] for earlier comments).

The Cosmic Microwave Background (CMB) dipole is almost ubiquitously assumed to be kinematic in origin, i. e. due to relative motion. By subtracting the dipole, the CMB is defined as the rest frame for the Universe. Some of the CMB anomalies have been documented in [12] and refer to anomalies with directional dependence, for example the (planar) alignment of the quadrupole and octopole and their normals with the CMB dipole [13, 14]. In addition, it has been argued that an anomalous parity asymmetry [15] may be traced to the CMB dipole [16, 17], so a common origin for CMB anomalies is plausible.

Separately, attempts to recover the CMB dipole from counts of late Universe sources such as radio galaxies [18–25] and QSOs [26], which are assumed to be in "CMB frame", largely agree that the CMB dipole direction is recovered, *but not the magnitude*. The implication is that observables in the late Universe are not in the same FLRW Universe. Independently, similar findings have emerged from studies of the apparent magnitudes of Type Ia supernovae (SN) [27] and QSOs [28]. In contrast, analysis of higher CMB multipoles confirms the CMB dipole magnitude [29].[1] It should be stressed that although the statistics may be impressive, these results are based on partial sky coverage and this is an important systematic.

Without doubt, the bread and butter of FLRW cosmology is the Hubble parameter $H(z)$. In particular, Hubble tension [1–5] casts a spotlight on $H_0 = H(z = 0)$. Here, we build on earlier observations for strongly lensed QSOs [10] and Type Ia SN [34] that H_0 values in the direction of the CMB dipole, loosely defined, are larger. Similar variations of H_0 across the sky have been reported for scaling relations in galaxy clusters [35, 36].[2] Note, within FLRW the value of H_0 is insensitive to the number of observables in any given direction, but of course the number of observables impacts the errors. Finally, a variation in H_0 across the sky recasts the Hubble tension discussion [1–5] as a symptom of a deeper issue.

Our findings are that QSOs and GRBs, on the assumption that they represent *standardisable candles* [37–47], return higher H_0 values in hemispheres aligned with the CMB dipole direction. See also [48] for overlapping analysis. Admittedly, in contrast to Type Ia SN, QSOs and GRBs are non-standard, but *if* they are merely good enough to track H_0, namely a universal constant in *all* FLRW cosmologies, then we arrive at results that contradict FLRW. The physics of strong lensing time delay, Type Ia SN, QSOs and GRBs are sufficiently different with different systematics. It is hence plausible that the Universe is anisotropic. As explained in [10], future observations of strongly lensed QSOs [49, 50] and potentially lensed SN [51] may settle the issue to everyone's satisfaction.

*Electronic address: orlando.luongo@unicam.it
†Electronic address: muccino@lnf.infn.it
‡Electronic address: eoin@sogang.ac.kr
§Electronic address: shahin.s.jabbari@gmail.com
¶Electronic address: yinlu@sogang.ac.kr

[1] Interesting spatial dependence in the fine structure constant [30, 31] and alignments in QSO polarisations [32, 33] have been reported elsewhere. The latter define an axis closely aligned with the CMB dipole.

[2] Curiously, [35, 36] find that H_0 is lower along the CMB dipole direction, but restrict Ω_m to a Planck value in the analysis. This difference is worth investigating.

II. QSO DATA

QSOs as standardisable candles in cosmology would be a game changer, since they are plentiful even up to redshift $z \sim 7$. Despite a number of competitive proposals, e. g. [52–54], arguably the simplest approach, due to Risaliti & Lusso [47], exploits an empirical relation between X-ray and UV luminosities in QSOs [55],

$$\log_{10} L_X = \beta + \gamma \log_{10} L_{UV}, \tag{1}$$

where β and $\gamma \approx 0.6$ are constants. Various studies have shown the robustness of the slope γ over both orders of magnitude in luminosity and extended redshift ranges [56–59]. The program [47, 60–62] is still in its infancy and reminiscent of the status of Type Ia SN in the 1990s [63]. The results so far have been intriguing, especially since they are at odds with Planck-ΛCDM [8]. In particular, QSOs (and GRBs) prefer larger values of matter density Ω_m, consistent with a Universe with little or no dark energy [64–67].[3] This is due to a preference within QSOs for lower luminosity distances $D_L(z)$ relative to Planck-ΛCDM [8], especially at higher redshifts. Lastly, it has been argued that best fit values of β, γ may be sensitive to the cosmological model, suggesting they should only be employed over restricted redshift ranges [72] or with QSO subsamples [73].

Evidently, a large Ω_m causes the most immediate concern. However, this is an inference within flat ΛCDM and the latter is under scrutiny [1–7]. Note also that SN become sparse above $z = 1$, so the waters are largely uncharted, and we are reliant on QSO and Lyman-α BAO for guidance. Tellingly, earlier determinations of Lyman-α BAO [69] were discrepant with Planck-ΛCDM, but the discrepancy has reduced in recent years [71]. More recently, DES announced BAO results through a blinded analysis at an effective redshift of $z = 0.835$, which are in tension with Planck-ΛCDM at 2.3σ [70]. The reader should observe that late time cosmology beyond $z \sim 1$ is far from settled. It is wise to keep an open mind.

A. Methods

The key idea of Risaliti & Lusso [47] is to assume that the relation (1) holds, before converting it into a relation in UV and X-ray fluxes, F_{UV} and F_X, respectively:

$$\log_{10} F_X = \beta + \gamma \log_{10} F_{UV} + (\gamma - 1) \log_{10}(4\pi D_L^2). \tag{2}$$

In a flat cosmology $D_L(z)$ may be expressed as

$$D_L(z) = c(1+z) \int_0^z \frac{1}{H(z')} \mathrm{d}z'. \tag{3}$$

[3] As explained in [68], the results of [60–62] have been negatively impacted by the cosmographic expansion, so claims of discrepancies in Ω_m cannot be substantiated without outside analysis.

Owing to the scatter in the QSO data, an additional intrinsic dispersion parameter δ is considered [47]. Thus, within the flat ΛCDM model, in addition to two cosmological parameters, (H_0, Ω_m), there are three extra parameters: β, γ from (2) and δ. However, H_0 is degenerate with β, so both cannot be independently determined without external data. Here we do not combine data sets, as the poorer quality QSO data risks returning unrepresentative values [64] and the goal is to extract information from QSOs directly. Therefore, we fix H_0 to the canonical value $H_0 = 70$ km/s/Mpc and fit β as a proxy for H_0. As should be clear from equation (2), since $\gamma \approx 0.6 < 1$, an *increase* in β maps over into an *increase* in H_0.

The best-fit parameters $(\Omega_m, \beta, \gamma, \delta)$ follow from extremising the likelihood function [47],

$$\mathcal{L} = -\frac{1}{2} \sum_{i=1}^{N} \left[\frac{\left(\log_{10} F_{X,i}^{\text{obs}} - \log_{10} F_{X,i}^{\text{model}}\right)^2}{s_i^2} + \ln(2\pi s_i^2) \right], \tag{4}$$

where $s_i = \sigma_i^2 + \delta^2$ contains the measurement error on the observed flux $\log_{10} F_{X,i}^{\text{obs}}$ and δ. $\log_{10} F_{X,i}^{\text{model}}$ carries information about the cosmological model through (2).

On the data side, we make use of the latest compilation of QSO data [62], which contains 2421 QSOs in the redshift range $0.009 \leq z \leq 7.5413$. We show the redshift distribution of the QSOs and their distribution on the sky in FIG. 1 and FIG. 2. Evidently, the data becomes sparse as one approaches $z = 4$, while it is noticeable that the majority of the QSOs, 1655 in fact, are located in the range $90^\circ < \text{RA} < 270^\circ$ and in the northern hemisphere, DEC $> 0^\circ$. As explained in [62], while one can use the overall data set, the UV fluxes for some $z < 0.7$ QSOs have been determined by extrapolation from the optical, however there are some local QSOs, $z < 0.1$, whose UV spectra have been determined without extrapolation and one can have greater confidence in them. While one can include the local QSOs, it is conservative to remove all the QSOs below $z = 0.7$ [62] and this reduces the sample to 2023 QSOs. Observe that $z = 0.7$ is large enough that all the QSOs are expected to be in the same FLRW Universe as the CMB. Peculiar velocities are not relevant.

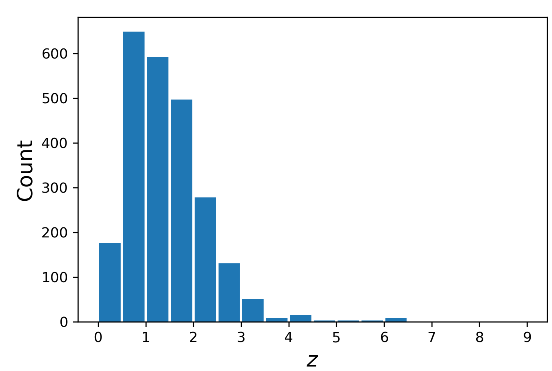

FIG. 1: The redshift distribution of the 2421 QSOs from the recent compilation [62] in intervals of $\Delta z = 0.5$.

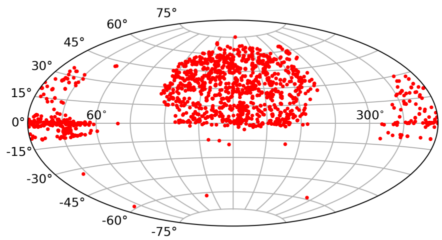

FIG. 2: Distribution of the QSOs [62] on the sky.

B. Analysis

We start by performing a consistency check in a bid to recover results quoted in [72]. To that end, we retain the local QSOs, $z < 0.1$, which we combine with QSOs in the redshift range $0.7 < z < 1.479$.[4] Throughout we use the flat priors $0 \leq \Omega_m \leq 1$, $0 < \beta < 15$, $0 < \gamma < 1$ and $0 < \delta < 1$. As is clear from Table I, the results of extremisation and MCMC agree well, modulo the fact that Ω_m is displaced to smaller values. We have checked that the best-fit Ω_m value corresponds to the peak of the distribution, at least within the bounds, which means once restricted to the range $0 \leq \Omega_m \leq 1$, the distribution is lopsided, so the percentiles are shifted to smaller values. In effect, Ω_m wants to exceed the bound in order to reduce $D_L(z)$, but within flat ΛCDM, it cannot. Thus, displacements in MCMC values of Ω_m are an artefact of the bounds, otherwise extremisation and MCMC show good agreement. Finally, we can compare the results from [72], reproduced in Table I and confirm that there is agreement, despite a slight difference in data (see footnote 4).

Ω_m	β	γ	δ
0.843	9.110	0.589	0.238
$0.697^{+0.204}_{-0.238}$	$8.980^{+0.505}_{-0.531}$	$0.594^{+0.017}_{-0.016}$	$0.239^{+0.006}_{-0.006}$
0.800	8.695	0.584	0.238
$0.670^{+0.300}_{-0.130}$	$8.570^{+0.530}_{-0.530}$	$0.588^{+0.018}_{-0.018}$	$0.239^{+0.006}_{-0.006}$

TABLE I: The best-fit values of the parameters for QSOs in the redshift range $z < 0.1 \cup 0.7 < z < 1.479$. The first line corresponds to extremising the likelihood (4), whereas the second follows from an MCMC exploration, where we quote 1σ confidence intervals. The third and fourth lines record the analogous results from [72], modulo a slight difference in data (footnote 4).

The take away from the warmup exercise is that both extremisation and MCMC return consistent values of β. For us this is important, as we will explore variations of β across the sky by scanning over RA, DEC and using extremisation to identify differences in absolute β values between hemispheres. This is considerably quicker than MCMC, or fitting the logarithm dressed H_0, and once the variations in β have been identified, we drill down on the more interesting orientations using MCMC in order to quantify the errors and extract the significance of any discrepancy. Concretely, we break the sky up into a 31×15 grid. Each point on this grid corresponds to two angles, which can be traded for a vector [34],

$$\vec{v} = [\cos(\mathrm{DEC})\cos(\mathrm{RA}), \cos(\mathrm{DEC})\sin(\mathrm{RA}), \sin(\mathrm{DEC})]. \quad (5)$$

Observe that one gets the antipodal point on the sky by flipping the sign of DEC and shifting RA by 180°, so by opting for an odd number of points in our grid, we include antipodal points. This duplication allows a key consistency check. Next, one separates the sample based on the sign of the inner product of this vector with the corresponding vector for each data point in the QSO sample. This splits the data into two hemispheres. Once done, one extremises the likelihood (4) for each hemisphere and records the difference between the "northern" (N) and "southern" (S) hemisphere, $\Delta\beta = \beta^N - \beta^S$.

The result of this scan over the angles is shown in FIG. 3, where we have included the CMB dipole direction $(\mathrm{RA}, \mathrm{DEC}) = (168°, -7°)$ for guidance, and used the python library *scipy* (scipy.interpolate.griddata) to perform a cubic interpolation in $\Delta\beta$. We have checked that, as it is also visible in Fig. 3 or Fig. 4, the antipodal point on the sky simply flips the sign of $\Delta\beta$. For this reason, the mean (and median) of our distribution in $\Delta\beta$ coincides with $\Delta\beta = 0$ and we have confirmed this is the case. In Table II we record the best-fit parameters for the CMB dipole direction and the direction of maximum $\Delta\beta$, where we have suppressed δ as it shows little variation. Note, we only consider the maximum $\Delta\beta$ from the sampled points and not the interpolation.

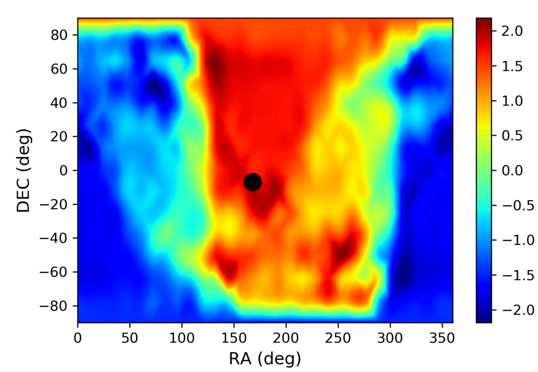

FIG. 3: Variations of the best-fit β parameters in respective hemispheres as (RA, DEC) values for the QSOs in the redshift range $0.7 < z \leq 7.5413$. The black dot denotes the CMB dipole. The lower (higher) β region corresponds to lower (higher) H_0 regions.

As is clear from Table II, once again extremisation and MCMC show good agreement. We have randomly sampled other points to confirm that this agreement is more widespread. From the 1σ confidence intervals in Table II one

[4] In the data set downloaded from VizieR, we are unable to find the last two entries in Table 2 of [62], otherwise we are using the same local QSOs.

(RA, DEC)	Hemisphere	Ω_m	β	γ
CMB dipole	N	1	8.491	0.609
		$0.924^{+0.057}_{-0.107}$	$8.451^{+0.356}_{-0.371}$	$0.610^{+0.012}_{-0.011}$
	S	1	6.787	0.663
		$0.880^{+0.087}_{-0.155}$	$6.714^{+0.535}_{-0.538}$	$0.666^{+0.017}_{-0.017}$
$(132°, 64.3°)$	N	1	8.474	0.609
		$0.934^{+0.048}_{-0.096}$	$8.426^{0.354}_{-0.343}$	$0.611^{+0.011}_{-0.011}$
	S	1	6.291	0.679
		$0.845^{+0.114}_{-0.191}$	$6.171^{+0.633}_{-0.594}$	$0.683^{+0.019}_{-0.020}$

TABLE II: Best-fit values of the parameters from both extremisation and MCMC analysis of the likelihood (4) for QSOs in the redshift range $0.7 < z \leq 7.5413$.

can estimate the discrepancy in $\Delta\beta$ between hemispheres to be 2.7σ for the CMB dipole and 3σ for the maximum $\Delta\beta$. It is easy to check that both directions are in the same hemisphere using the vector inner product. These results may not be so surprising since we are working with the same tracer (QSOs) where a mismatch in the cosmic dipole has been reported with the CMB dipole at $\sim 5\sigma$ [26]. From our end, FIG. 3 is reminiscent of similar features in strong lensing time delay [10] and Type Ia SN [34].

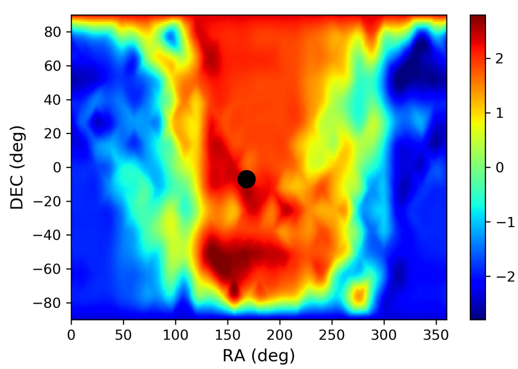

FIG. 4: Variations of the best-fit β parameters in respective hemispheres as (RA, DEC) values for the QSOs in the redshift range $0.7 < z < 1.7$. The black dot denotes the CMB dipole.

It remains to address caveats. There are concerns that β evolves with redshift [72] (see Table 3). From results therein, it is clear that β is robust through to $z \sim 2.25$, but combining low and high redshift QSOs can lead to inconsistent values. We confirm this mistmatch in appendix A, but conclude that any evolution beyond $z = 1.7$ (versus $z = 1.479$ [72]) is not significant. However, it is prudent to repeat our analysis in the more conservative range $0 < z < 1.7$. The resulting plot and results can be found in FIG. 4 and Table III. As expected, with the restricted redshift range, we reduce the QSO count to 1255, so this inflates the errors and reduces the significance. That being said, we still find a 2σ discrepancy for the CMB dipole and 2.8σ for the maximum $\Delta\beta$. Once again, these directions are in the same hemisphere. Interestingly, the maximum $\Delta\beta$ direction has flipped hemisphere, but this may be expected: FLRW H_0 is an extremely blunt probe of any anisotropy. Nevertheless, qualitatively FIG. 4 is the same as FIG. 3.

(RA, DEC)	Hemisphere	Ω_m	β	γ
CMB dipole	N	1	9.527	0.575
		$0.694^{+0.211}_{-0.261}$	$9.435^{+0.589}_{-0.573}$	$0.579^{+0.018}_{-0.019}$
	S	1	7.604	0.636
		$0.762^{+0.168}_{-0.273}$	$7.489^{+0.805}_{-0.788}$	$0.641^{+0.025}_{-0.026}$
$(132°, -51.4°)$	N	0.678	11.199	0.524
		$0.587^{+0.283}_{-0.294}$	$11.084^{+0.898}_{-0.917}$	$0.528^{+0.030}_{-0.028}$
	S	1	8.206	0.617
		$0.806^{+0.139}_{-0.214}$	$8.121^{+0.537}_{-0.563}$	$0.620^{+0.018}_{-0.017}$

TABLE III: Best-fit values of the parameters from both extremisation and MCMC analysis of the likelihood (4) for QSOs in the redshift range $0.7 < z < 1.7$.

Another caveat/feature is that our analysis rests exclusively upon flat ΛCDM. Since the QSO data returns large values of Ω_m, it is expected that changes in the dark energy model, which primarily affect low redshifts, do not affect β, γ and this can be confirmed from Table 3 of ref. [72]. In particular, observe that β errors do not increase as the model changes, which implies that the significance of the deviation we see in flat ΛCDM will not change across dark energy models. However, introducing curvature Ω_k causes β to jump as is clear from a comparison of the "Flat ΛCDM" and "Non-flat ΛCDM" entries in Table 3 [72]. But this can be readily explained. As discussed, QSOs prefer smaller $D_L(z)$ than Planck-ΛCDM. However, when one introduces curvature Ω_k, for $\Omega_k < 0$, a sine function appears in the definition of $D_L(z)$, see e.g. eq.(9) of [72], which is bounded above by unity. Thus, QSO data can exploit this bound to saturate to lower $D_L(z)$ values. This can lead to turning points in $H(z)$, as is clear from some of the results in [72].[5] The jump in β can nonetheless be simply explained by the additional freedom beyond Ω_m that the data has to reduce $D_L(z)$, and increase $H(z)$, at higher z.

Caveats aside, we are seeing strong evidence for a higher value of H_0 within the flat ΛCDM model in the direction of the CMB dipole or aligned directions. Since we treat both hemispheres equally, there is no obvious bias. Indeed, FIG. 3 and FIG. 4 are reminiscent of similar features in strong lensing time delay [10] and Type Ia SN [34]. The naive interpretation is that there is an anisotropy in the matter density of the Universe as traced by QSOs. This is consistent with the observation that there is a mismatch in the magnitude of the cosmic dipole between QSOs and CMB [26], but here (partial) sky coverage is not a concern.

[5] See [74] for comments on turning points in $H(z)$ and implications for the Null Energy Condition.

III. GRBS

Our complementary analysis here is guided by the findings in [75], where assuming the Amati correlation [39], a compilation of 118 GRBs in the redshift range $0.3399 \leq z \leq 8.2$ with small enough intrinsic dispersion was identified. The relatively low scatter suggests that this sample may currently be the most suitable sample for cosmological studies. Given the improvement relative to previous samples, e. g. [76], it is interesting to see if GRBs, which are also high redshift probes, show the same feature as QSOs.

Recall that the Amati correlation relates the spectral peak energy in the GRB cosmological rest-frame $E_{\rm p,i}$ and the isotropic energy $E_{\rm iso}$:

$$\log_{10} E_{\rm iso} = \alpha + \beta \log_{10} E_{\rm p,i}, \tag{6}$$

where α and β are free parameters. Neither $E_{\rm iso}$ nor $E_{\rm p,i}$ are observed quantities. The latter is related to the similar quantity in observer's frame as $E_{\rm p,i} = E_{\rm p}^{\rm obs}(1+z)$ and the former depends on the cosmology through the luminosity distance $D_L(z)$ and the measured bolometric fluence $S_{\rm bolo}$ [76],

$$E_{\rm iso} = 4\pi D_L^2(z) S_{\rm bolo}(1+z)^{-1}. \tag{7}$$

Once again we focus on flat ΛCDM and to address scatter in the GRB data, an intrinsic dispersion parameter δ is introduced. In line with previous analysis, we fix $H_0 = 70$ km/s/Mpc and adopt Ω_m, α, β and δ as the free parameters. The best-fit values are identified by extremising the following likelihood function:

$$\mathcal{L} = -\frac{1}{2}\sum_{i=1}^{N}\left[\frac{\left(\log_{10} E_{{\rm iso},i} - (\alpha + \beta \log_{10} E_{{\rm p},i})\right)^2}{s_i^2} + \ln(2\pi s_i^2)\right], \tag{8}$$

where N is the number of GRBs. In addition, s_i depends on the $S_{\rm bolo}, E_{\rm p,i}$, the corresponding errors $\sigma_{S_{\rm bolo}}, \sigma_{E_{\rm p,i}}$ and the intrinsic dispersion,

$$s_i^2 = \left(\frac{\sigma_{S_{{\rm bolo},i}}}{S_{{\rm bolo},i}\ln(10)}\right)^2 + \beta^2\left(\frac{\sigma_{E_{{\rm p},i}}}{E_{{\rm p},i}\ln(10)}\right)^2 + \delta^2 \tag{9}$$

We see from equation (6) that the degeneracy between H_0 and α means that an *increase* in H_0 corresponds to a *decrease* in α. Therefore, relative to QSOs, the degeneracy is opposite.

The methodology is the same as section II and the result of the scan over (RA, DEC) can be found in FIG. 7 and Table IV, where we record best-fit parameters for the CMB dipole direction and the direction of least $\Delta\alpha$. We suppress δ in Table IV as it consistently returns values in the vicinity of $\delta \approx 0.4$. Given we have an order of magnitude fewer GRBs, it is not surprising to see that any deviation in $\Delta\alpha$ is not so pronounced. From Table IV, we find that the discrepancy in α across hemispheres is 0.5σ for the CMB dipole and 1.6σ for the direction of minimum $\Delta\alpha$ (maximum ΔH_0). Once again both vectors are in the same hemisphere and it is clear from the naked eye that FIG. 7 and 3 show similar regions on the sky where H_0 increases. Owing to the small size of the GRB sample, we do not consider restricted redshift ranges.

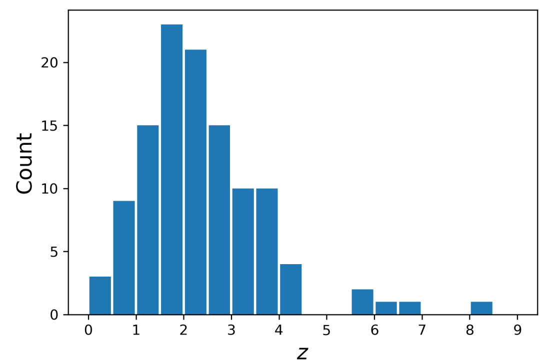

FIG. 5: Distribution of 118 GRBs with redshift z in intervals of $\Delta z = 0.5$.

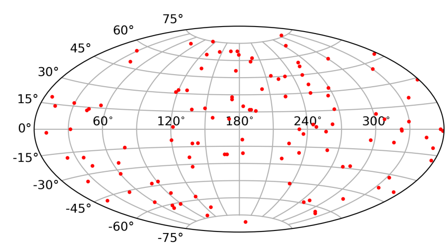

FIG. 6: Distribution of the GRBs on the sky.

However, given the size of the GRB sample, it is admittedly a little surprising that FIG. 7 shows such good qualitative agreement with FIG. 3. In appendix B, we repeat the exercise with a sample of 162 GRBs with greater scatter [76], and show that while H_0 is in fact *smaller* in the CMB dipole direction with the full sample, when one focuses on subsamples

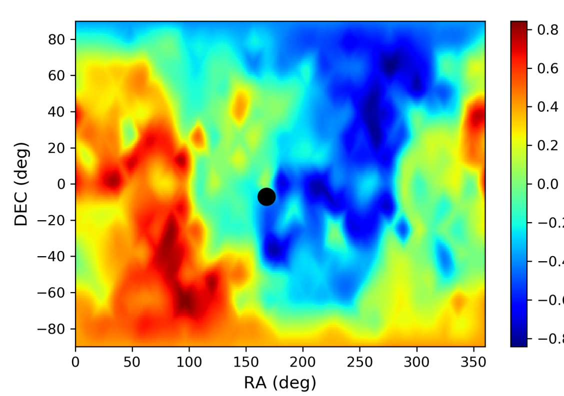

FIG. 7: Variations of the best-fit α parameter in respective hemispheres as (RA, DEC) values for the GRBs are scanned over. The black dot denotes the CMB dipole. Note that a higher (lower) value α corresponds to lower (higher) value H_0.

that more closely follow the best fit cosmology, one arrives at consistent results. Therefore, we expect that scatter in smaller data sets may obscure what we believe is a general trend.

Let us make one final comment. Our results here are based on real GRB data. Separately, we have performed simulations that assume only the Amati relation and a distribution for the data representative of the 118 GRB sample. Observe that the Amati relation assumes FLRW. From the distributions, it is an easy task to generate mock samples of 300 and 1000 GRBs before repeating the steps of our analysis by fitting the flat ΛCDM model. Unsurprisingly, we find that with smaller mock samples, features such as those in FIG. 7 routinely arise as statistical fluctuations, but for 1000 GRBs we find no such features. While the result is expected, the exercise is interesting, since the mocks are not performed within flat ΛCDM, but within the more general setting of a relation that assumes FLRW. Thus, FIG. 7 is expected to be only discrepant with a flat ΛCDM Universe at 1.5σ, at least based on similar simulations performed in [34], but it may represent a fluke in a more general FLRW Universe. Simply put, we currently do not have enough real GRBs to make definitive statements based on GRB data alone.

(RA, DEC)	Hemisphere	Ω_m	α	β
CMB dipole	N	1	49.83	1.17
		$0.67^{+0.23}_{-0.30}$	$49.91^{+0.40}_{-0.36}$	$1.20^{+0.13}_{-0.15}$
	S	0.38	50.22	1.08
		$0.52^{+0.32}_{-0.27}$	$50.17^{+0.30}_{-0.28}$	$1.08^{+0.10}_{-0.10}$
$(264^\circ, +64.3^\circ)$	N	1	49.61	1.23
		$0.64^{+0.25}_{-0.30}$	$49.72^{+0.36}_{-0.34}$	$1.24^{+0.12}_{-0.12}$
	S	0.72	50.46	0.96
		$0.60^{+0.27}_{-0.29}$	$50.49^{+0.34}_{-0.34}$	$0.98^{+0.13}_{-0.12}$

TABLE IV: Best-fit values of the parameters from both extremisation and MCMC analysis of the likelihood (8) for GRBs in the redshift range $0.3399 \leq z \leq 8.2$. Note, we quote the minimum value of $\Delta\alpha$ corresponding to the maximum value of ΔH_0.

IV. DISCUSSION

Building on earlier observations in strong lensing time delay [10] and Type Ia SN [34], we find independent evidence in QSOs and GRBs that H_0 is larger in the CMB dipole direction or aligned directions. Note that we have simply assumed the flat ΛCDM model, which *a priori* has no directional preference and knows nothing about anisotropy. We focus on H_0, since H_0 is a universal constant in any FLRW cosmology. For this reason, one expects all trends to be robust across cosmological models, although significance may vary. The focus on H_0 also allows us to highlight H_0, the local value of which is the subject of ongoing debate [1–7], but if our findings hold up, then there is no reason for H_0 in an FLRW context to be unique. In essence, Hubble tension may not even make sense as a problem.

It is certainly worth noting that despite working with proxy constants that are degenerate with H_0, FIG. 3 and FIG. 7 negotiate signs to register good agreement across observables. Moreover, just as in the Hubble tension narrative, where one can replace H_0 with the absolute magnitude M_B of Type Ia SN [77, 78] to define "M_B tension", one has the same freedom with β and α here. Given the small sample of GRBs, they simply play an accompanying role, but the significance of the deviation in the QSOs across the whole sample [62] is $\sim 3\sigma$. Importantly, our lowest redshift QSO and GRB are sufficiently deep in redshift that all the data is expected to share the same FLRW background as the CMB frame.

Obviously, both QSOs and GRBs are not widely used in cosmology, although this is changing in recent years [79–95]. Both have great potentials as they probe redshift ranges not accessible by other probes. Nonetheless, they come with caveats, and of course, as we have shown here, when working with the latest QSO compilation [62], one is implicitly working with a data set that is not only at odds with flat ΛCDM (large Ω_m), but also FLRW. As argued, this high redshift window in the late Universe is largely unexplored and even BAO has led to curious results [69, 70], so it is imperative to maintain an open mind. One can either increase Ω_m or introduce a large negative Ω_k [72] to reduce $D_L(z)$, since the dark energy sector is irrelevant. However, when one introduces negative Ω_k, care is required with turning points in $H(z)$ which brings in its own issues [74]. In general with a new avenue to reduce $D_L(z)$, i. e. Ω_k in addition to Ω_m, some jump in the parameters (β, γ) may be expected.

Summing up, the results of [72, 73] suggest that QSOs return consistent values of (β, γ) out beyond $z = 2$, but there are some curious inconsistencies currently, namely jumps in parameters, when one uses all the data in the most recent compilation [62]. That being said, our analysis in the redshift range $0.7 < z < 1.7$ should be safe from these caveats, and in the appendix, we show that evolution beyond $z = 1.7$ may be marginal, in line with earlier studies [56–59]. It should be stressed again that we have not employed any ansatz to guide the data, but simply worked within flat ΛCDM, so the observation that H_0 is higher across i) strong lensing time delay [10], ii) Type Ia SN [34], iii) QSOs and iv) GRBs, surely must have some interesting physical explanation. Obviously, an anisotropic Universe is the simplest interpretation and this claim can be tested by any competitive cosmological data set going forward. We have a prediction and as we gather more and better quality data the claim can either be true or false, but community engagement is required.

We close by briefly discussing the theoretical ramifications of our results. If further data confirms our findings, the simplest explanation may be that we have a preferred direction, aligned with the CMB dipole, in the Universe. That is, going to CMB rest-frame we see an anisotropic background. Homogeneous but anisotropic cosmologies are classified by Bianchi models. Since flat ΛCDM is apparently already a good approximation to the Universe, such Bianchi models should be anisotropic deviations from the flat ΛCDM. Moreover, our findings require the presence of a preferred "dipole" direction, which may be found in specific Bianchi models, such as the "tilted cosmology" of King and Ellis [96, 97]. Going beyond FLRW, one should revisit all the cosmological analyses and inferences, and write a new chapter in the cosmology book.

Acknowledgements

We thank Stephen Appleby, Narayan Khadka, Bharat Ratra and Jian-Min Wang for helpful discussions. We are grateful to Mohamed Rameez and Jenny Wagner for comments on a preliminary draft. We especially thank Chethan Krishnan and Roya Mohayaee for ongoing discussions on related topics. EÓC is funded by the National Research Foundation of Korea (NRF-2020R1A2C1102899). MMShJ would like to acknowledge SarAmadan grant No. ISEF/M/400122. LY was supported by the National Research Foundation of Korea funded through the CQUeST of Sogang University (NRF2020R1A6A1A03047877). OL and MM acknowledge the Ministry of Education and Science of the Republic of Kazakhstan, Grant: IRN AP08052311.

Appendix A: Low z & high z mismatch

In the body of the paper, we have explained how spatial curvature can be exploited to reduce $D_L(z)$ at higher redshifts within the FLRW cosmologies. Understandably, if data has two knobs to dial, i. e. Ω_m and Ω_k, it can find points in the parameter space of relation (1) that may not be accessible with only one parameter. For this reason, the jump in (β, γ) with curvature reported in [72] does not concern us too much, as first one has to motivate a large value for Ω_k and ensure that there are no unphysical turning points in $H(z)$, which would signal a breakdown in the Null Energy Condition [74].

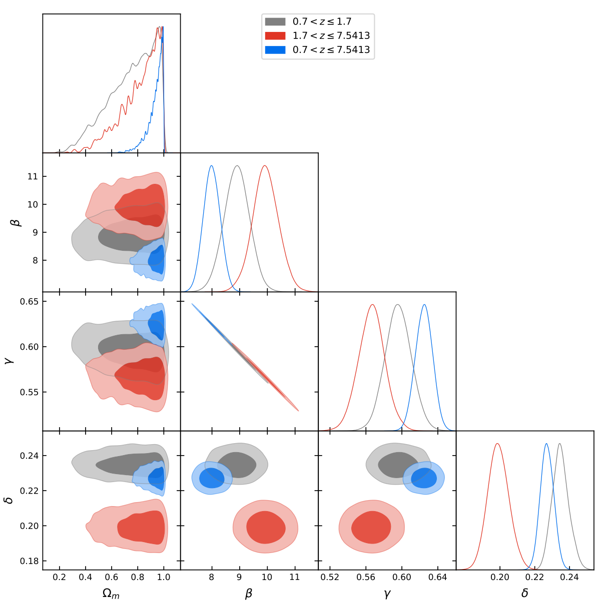

FIG. 8: Differences in the parameters Ω_m, β, γ and δ between low and high redshift samples. Here we made use of *getdist* [98].

More concerning is the observation within flat ΛCDM that low and high redshift QSOs lead to inconsistent values when combined. Using the redshift $z = 1.7$ (in contrast to $z = 1.479$ [72]) as the border between low and high z, we confirm this in FIG. 8. Evidently, the red (high z) region may be marginally discrepant with grey (low z), but our cut-off $z = 1.7$ is low enough that the grey and blue regions (all z) are more or less consistent. Interestingly, the intrinsic dispersion δ drops considerably at higher redshifts, and since this shrinks the errors, the linear relation (1) should become more sensitive to scatter in the data. This lower δ at higher redshift is also evident in Table 3 of [72]. That being said, there is no glaring inconsistency between grey and blue regions, so we are optimistic that both FIG. 3 and FIG. 4 are tracking H_0 appropriately. Whether QSOs can constrain the normalised Hubble parameter $E(z)$, or not, is a separate matter that interests us less.

Appendix B: Comments on robustness

Given the small size of the GRB sample [75] and the scatter in the data, it may come as a surprise to the reader that FIG. 7 shows such good qualitative agreement with FIG. 3 once the implications for H_0 are unravelled. The claim of [75] is that this sample is optimal for cosmology, since it has less scatter than other samples in the literature. Of course, going forward it is imperative to test other data sets, and even data sets beyond GRBs, and for that reason it is instructive to illustrate how our GRB findings would change with another representative data set. Thus, here we make use of the sample of 162 GRBs in the redshift range $0.03351 \leq z \leq 9.3$ [76], where the distance moduli μ have been calibrated using Type Ia SN. Observe that there are no nuisance parameters, e. g. α, β, δ, and we can directly fit (H_0, Ω_m) to the distance moduli.

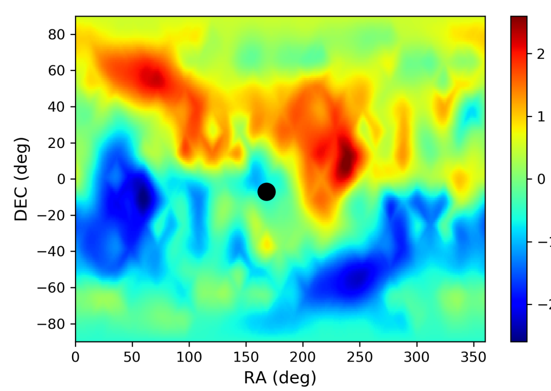

FIG. 9: Variations of (B1) across the sky for the 162 GRB of [76].

Repeating the process outlined in the text with the full data set, while focusing on the quantity [34],

$$\sigma := (H_0^N - H_0^S)/\sqrt{(\delta H_0^N)^2 + (\delta H_0^S)^2}, \tag{B1}$$

one arrives at FIG. 9. Note that in contrast to plots in the text, here the colour map is recording the significance of the discrepancy and not just the discrepancy. Obviously, this plot shows little or no correlation and is inconclusive. Moreover, in the CMB dipole direction H_0 is actually lower, thus contradicting our hypothesis. Nevertheless, we are encountering $\sim 2\sigma$ displacements at certain points on the sky.

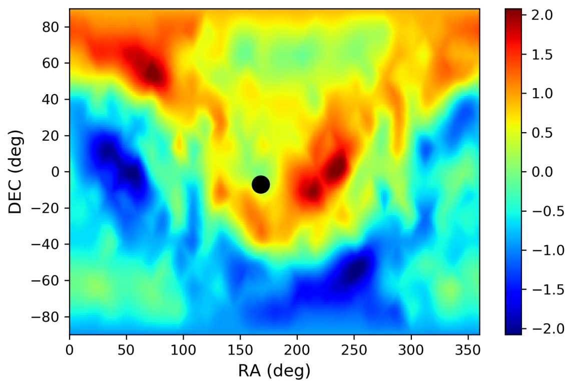

FIG. 10: Variations of (B1) across the sky for a 137 GRB subsample of the 162 GRBs of [76]. We have reduced the scatter by removing GRB data with larger residuals with respect to the best-fit cosmology.

However, let us remove some of the GRBs by hand with the specific goal of reducing scatter in the data. To do this, we simply impose a cut-off on the residuals from the best-fit flat ΛCDM cosmology of the overall sample of 162 GRBs. One can focus on the data points themselves since the errors are pretty uniform (see Table 4 of [76]). Defining the distance modulus $\mu(z) := 25 + 5\log_{10}[D_L(z)/\text{Mpc}]$, we first remove GRBs that are beyond $\Delta\mu = 1.5$ from the best-fit flat ΛCDM cosmology, $H_0 = 70.3 \pm 9.5$ km/s/Mpc, $\Omega_m = 0.41 \pm 0.22$. This leaves us with 137 GRBs with consistent values of (H_0, Ω_m), but smaller residuals. The corresponding plot for this smaller sample can be found in FIG. 10. The CMB dipole is now clearly enclosed by a region where H_0 is higher and by fitting the data for the CMB dipole direction, we confirm that H_0 is marginally higher in this direction. Finally, we reduce the sample to 106 GRBs by rejecting all data points where $\Delta\mu > 1$. Doing so, we find FIG. 11, where the CMB dipole direction is neatly enclosed in a region on the sky where H_0 is higher. In the CMB dipole direction, H_0 is 1.3σ higher and the maximum discrepancy is 2.1σ in the direction (RA,DEC) $= (216^\circ, 12.9^\circ)$. As one will observe, traces of this direction were there in the initial FIG. 9.

Let us try to summarise the lessons learned. First, as one ventures beyond Type Ia SN one finds data sets with potential applications to cosmology with considerably greater intrinsic scatter. On its own this is not a problem, since our understanding of Type Ia has evolved considerably in the last two decades. Recall that when dark energy was discovered, there was no correction for shape or colour of the light curve. In large data sets, e. g. QSOs, it is possible that the shear weight of statistics can overcome this scatter, whereas in GRBs this is not guaranteed. As a result, it is surprising that we get such a strong signal for an emergent dipole in FIG. 7. Here we have shown that this is not guaranteed. Nevertheless, as we see if

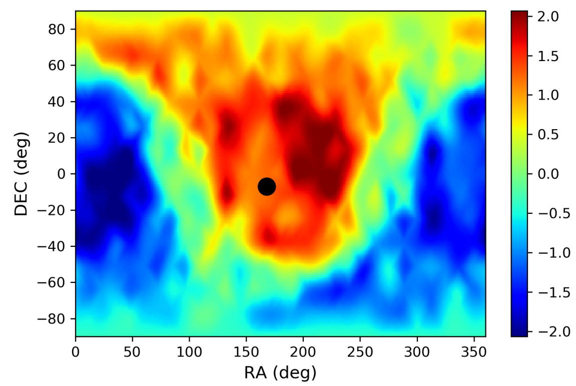

FIG. 11: Variations of (B1) across the sky for a 106 GRB subsample of the 162 GRBs of ref. [76]. We have reduced the scatter by removing GRB data with larger residuals with respect to the best-fit cosmology.

one focuses on data with the smallest residuals, namely the data that follows the underlying cosmology the best, one can get a definitive signature. The key point is that any trends in H_0 may be there, only that they may be hidden by the intrinsic scatter. Finally, it is worth stressing again that the GRB distance moduli here have been calibrated using SN Ia. However, angular distribution over the sky never features when one calibrates GRB data and one only employs redshifts. Therefore, our result on H_0 variation over the sky from the GRBs is independent of a similar variation based on the SN Ia Pantheon data set reported in [34].

Appendix C: Data

We record the GRB data compiled earlier in [75] in the below table. The QSO data [62] can be downloaded from https://vizier.u-strasbg.fr/viz-bin/VizieR?-source=J/A+A/642/A150.

TABLE V: The GRB data points

Name	**Redshift** z	E_p	S_{bolo}	**RA**	**DEC**
080916C	4.35	6953.87 ± 1188.77	10.40 ± 0.24	119.88	-57
090323	3.57	2060.09 ± 138.07	15.76 ± 0.39	190.69	17
090328	0.736	1221.71 ± 81.87	7.99 ± 0.20	90.87	-42
090424	0.544	236.91 ± 4.55	5.72 ± 0.09	189.54	17
090902B	1.822	2146.57 ± 21.71	39.05 ± 0.22	265.00	27
090926A	2.1062	868.63 ± 13.85	17.90 ± 0.13	353.25	-39
091003A	0.8969	857.81 ± 33.08	4.43 ± 0.08	251.50	37
091127	0.49	60.32 ± 1.93	2.25 ± 0.04	36.57	-19
091208B	1.063	202.63 ± 20.10	0.75 ± 0.04	29.41	17
100414A	1.368	1370.82 ± 27.68	11.88 ± 0.16	183.62	20
100728A	1.567	797.62 ± 18.05	11.74 ± 0.17	77.07	-14
110721A	3.512	8675.78 ± 852.66	6.14 ± 0.09	333.40	-39
120624B	2.2	1214.47 ± 26.24	20.49 ± 0.25	170.94	9
130427A	0.3399	294.25 ± 5.86	31.72 ± 0.20	173.14	28
130518A	2.49	1601.40 ± 32.19	11.40 ± 0.11	355.81	48
131108A	2.40	1163.20 ± 28.54	4.85 ± 0.05	156.47	10

Name	redshift z	E_p	S_{bolo}	RA	DEC
131231A	0.6439	370.15 ± 4.97	17.42 ± 0.12	10.58	-2
141028A	2.33	1320.18 ± 50.90	4.89 ± 0.06	322.70	0
150314A	1.758	985.66 ± 13.20	9.20 ± 0.12	126.66	64
150403A	2.06	2428.51 ± 160.80	8.10 ± 0.17	311.50	-63
150514A	0.807	137.84 ± 14.93	0.71 ± 0.03	74.85	-61
160509A	1.17	19334.10 ± 652.25	49.91 ± 1.36	310.10	76
160625B	1.406	1546.86 ± 37.25	83.54 ± 1.16	308.27	7
170214A	2.53	2119.788 ± 119.06	22.40 ± 0.29	256.33	-2
170405A	3.51	1424.42 ± 35.24	9.24 ± 0.09	219.81	-25
971214	3.42	685.0 ± 133.0	0.87 ± 0.11	179.13	65
990123	1.6	1724.0 ± 466.0	35.80 ± 5.80	231.37	45
990510	1.619	423.0 ± 42.0	2.60 ± 0.40	204.53	-81
000131	4.5	987.0 ± 416.0	4.70 ± 0.80	93.39	-52
000926	2.07	310.0 ± 20.0	2.60 ± 0.60	256.06	52
010222	1.48	766.00 ± 30.0	14.6 ± 1.50	223.05	43
011211	2.14	186.0 ± 24.0	0.50 ± 0.06	168.82	-22
020124	3.2	448.0 ± 148.0	1.20 ± 0.10	143.28	-12
021004	2.3	266.0 ± 117.0	0.27 ± 0.04	6.73	19
030226	1.98	289.0 ± 66.0	1.30 ± 0.10	173.27	26
030323	3.37	270.0 ± 113.0	0.12 ± 0.04	166.53	-22
030328	1.52	328.00 ± 55.0	6.40 ± 0.60	182.69	-9
030429	2.65	128.0 ± 26.0	0.14 ± 0.02	183.28	-21
040912	1.563	44.00 ± 33.0	0.21 ± 0.06	359.00	-1
050318	1.44	115.00 ± 25.0	0.42 ± 0.03	49.68	-46
050401	2.9	467.0 ± 110.0	1.90 ± 0.40	247.88	2
050603	2.821	1333.0 ± 107.0	3.50 ± 0.20	39.98	-25
050820	2.612	1325.0 ± 277.0	6.40 ± 0.50	337.40	20
050904	6.29	3178 ± 1094.0	2.00 ± 0.20	13.67	14
050922C	2.198	415.0 ± 111.0	0.47 ± 0.16	317.39	-9
051109A	2.346	539.0 ± 200.0	0.51 ± 0.05	330.25	41
060115	3.53	285.0 ± 34.0	0.25 ± 0.04	54.05	17
060124	2.296	784.0 ± 285.0	3.40 ± 0.50	77.04	70
060206	4.048	394.0 ± 46.0	0.14 ± 0.03	202.95	35
060418	1.489	572.00 ± 143.0	2.30 ± 0.50	236.42	-4
060526	3.21	105.0 ± 21.0	0.12 ± 0.06	232.85	0
060707	3.425	279.0 ± 28.0	0.23 ± 0.04	357.08	-18
060908	2.43	514.0 ± 102.0	0.73 ± 0.07	31.83	0
060927	5.6	475.0 ± 47.0	0.27 ± 0.04	329.55	5
070125	1.547	934.00 ± 148.0	13.30 ± 1.30	117.85	31
071003	1.604	2077 ± 286	5.32 ± 0.590	301.85	11
071020	2.145	1013.0 ± 160.0	0.87 ± 0.40	119.66	33
080319C	1.95	906.0 ± 272.0	1.50 ± 0.30	258.98	55
080413	2.433	584.0 ± 180.0	0.56 ± 0.14	287.29	-28
080514B	1.8	627.0 ± 65.0	2.027 ± 0.48	322.82	-1
080603B	2.69	376.0 ± 100.0	0.64 ± 0.058	176.53	68
080605	1.6398	650.0 ± 55.0	3.40 ± 0.28	262.13	4
080607	3.036	1691.0 ± 226.0	8.96 ± 0.48	194.97	16
080721	2.591	1741.0 ± 227.0	7.86 ± 1.37	224.47	-12
080810	3.35	1470.0 ± 180.0	1.82 ± 0.20	356.78	0
080913	6.695	710.0 ± 350.0	0.12 ± 0.035	65.73	-25
081008	1.9685	261.0 ± 52.0	0.96 ± 0.09	279.99	-57
081028	3.038	234.0 ± 93.0	0.81 ± 0.095	121.89	2
081118	2.58	147.0 ± 14.0	0.27 ± 0.057	82.59	-43
081121	2.512	47.23 ± 1.08	1.71 ± 0.33	89.26	-61
081222	2.77	505.0 ± 34.0	1.67 ± 0.17	22.75	-34
090102	1.547	1149.00 ± 166.0	3.48 ± 0.63	128.26	33
090418	1.608	1567 ± 384	2.35 ± 0.59	269.33	33
090423	8.2	491.0 ± 200.0	0.12 ± 0.032	148.90	18
090516	4.109	971.0 ± 390.0	1.96 ± 0.38	138.27	-12
090715B	3.0	536.0 ± 172.0	1.09 ± 0.17	251.35	45
090812	2.452	2000.0 ± 700.0	3.08 ± 0.53	353.20	-11

Name	redshift z	E_p	S_{bolo}	RA	DEC
091020	1.71	280.0 ± 190.0	0.11 ± 0.034	175.72	51
091029	2.752	230.0 ± 66.0	0.47 ± 0.044	60.18	-56
100413	3.9	1783.60 ± 374.85	2.36 ± 0.77	266.00	16
100621	0.54	146.49 ± 23.9	5.75 ± 0.64	315.25	-51
100704	3.6	809.60 ± 135.70	0.70 ± 0.07	133.50	-24
100814	1.44	312.32 ± 48.8	1.39 ± 0.23	22.25	-18
100906	1.73	387.23 ± 244.07	3.56 ± 0.55	28.50	56
110205	2.22	740.60 ± 322.0	3.32 ± 0.68	164.50	68
110213	1.46	223.86 ± 70.11	1.55 ± 0.23	43.00	49
110422	1.77	421.04 ± 13.85	9.32 ± 0.02	111.75	75
110503	1.61	572.25 ± 50.95	2.76 ± 0.21	132.75	52
110715	0.82	218.40 ± 20.93	2.73 ± 0.24	237.50	-46
110731	2.83	1164.32 ± 49.79	2.51 ± 0.01	280.50	-29
110818	3.36	1117.47 ± 241.11	1.05 ± 0.08	317.25	-64
111008	5.0	894.00 ± 240.0	1.06 ± 0.11	60.25	-33
111107	2.89	420.44 ± 124.58	0.18 ± 0.03	129.25	-67
111209	0.68	519.87 ± 88.88	69.47 ± 8.72	14.25	-47
120119	1.73	417.38 ± 54.56	4.62 ± 0.59	120.00	-9
120326	1.8	129.97 ± 10.27	0.44 ± 0.02	273.75	69
120724	1.48	68.45 ± 18.60	0.15 ± 0.02	245.00	4
120802	3.8	274.33 ± 93.04	0.43 ± 0.07	44.75	14
120811C	2.67	157.49 ± 20.92	0.74 ± 0.07	199.71	62
120909	3.93	1651.55 ± 123.25	2.69 ± 0.23	275.50	-59
120922	3.1	156.62 ± 0.04	1.59 ± 0.18	234.75	-20
121128	2.2	243.20 ± 12.8	0.87 ± 0.07	300.50	54
130215	0.6	247.54 ± 100.61	4.84 ± 0.12	43.25	13
130408	3.76	1003.94 ± 137.98	0.99 ± 0.17	134.25	-32
130420A	1.3	128.63 ± 6.89	1.73 ± 0.06	196.10	59
130505	2.27	2063.37 ± 101.37	4.56 ± 0.09	137.00	17
130514	3.6	496.80 ± 151.8	1.88 ± 0.25	296.25	-8
130606	5.91	2031.54 ± 483.7	0.49 ± 0.09	249.25	30
130610	2.09	911.83 ± 132.65	0.82 ± 0.05	224.25	28
130612	2.01	186.07 ± 31.56	0.08 ± 0.01	259.75	-17
130701A	1.16	191.80 ± 8.62	0.46 ± 0.04	224.42	28
130831A	0.48	81.35 ± 5.92	1.29 ± 0.07	358.65	29
130907A	1.24	881.77 ± 24.62	75.21 ± 4.76	215.88	46
131030A	1.29	405.86 ± 22.93	1.05 ± 0.10	345.08	-5
131105A	1.69	547.68 ± 83.53	4.75 ± 0.16	71.01	-63
131117A	4.04	221.85 ± 37.31	0.05 ± 0.01	332.34	-32
140206A	2.73	447.60 ± 22.38	1.69 ± 0.03	145.35	67
140213A	1.21	176.61 ± 4.42	2.53 ± 0.04	105.22	-73

[1] A. G. Riess, S. Casertano, W. Yuan, J. B. Bowers, L. Macri, J. C. Zinn and D. Scolnic, Astrophys. J. Lett. **908** (2021) no.1, L6 [arXiv:2012.08534 [astro-ph.CO]].

[2] W. L. Freedman, [arXiv:2106.15656 [astro-ph.CO]].

[3] D. W. Pesce, J. A. Braatz, M. J. Reid, A. G. Riess, D. Scolnic, J. J. Condon, F. Gao, C. Henkel, C. M. V. Impellizzeri and C. Y. Kuo, *et al.* Astrophys. J. Lett. **891** (2020) no.1, L1 [arXiv:2001.09213 [astro-ph.CO]].

[4] J. P. Blakeslee, J. B. Jensen, C. P. Ma, P. A. Milne and J. E. Greene, Astrophys. J. **911** (2021) no.1, 65 [arXiv:2101.02221 [astro-ph.CO]].

[5] E. Kourkchi, R. B. Tully, G. S. Anand, H. M. Courtois, A. Dupuy, J. D. Neill, L. Rizzi and M. Seibert, Astrophys. J. **896** (2020) no.1, 3 [arXiv:2004.14499 [astro-ph.GA]].

[6] T. M. C. Abbott *et al.* [DES], [arXiv:2105.13549 [astro-ph.CO]].

[7] M. Asgari *et al.* [KiDS], Astron. Astrophys. **645** (2021), A104 [arXiv:2007.15633 [astro-ph.CO]].

[8] N. Aghanim *et al.* [Planck], Astron. Astrophys. **641** (2020), A6 [arXiv:1807.06209 [astro-ph.CO]].

[9] E. Di Valentino, O. Mena, S. Pan, L. Visinelli, W. Yang, A. Melchiorri, D. F. Mota, A. G. Riess and J. Silk, [arXiv:2103.01183 [astro-ph.CO]].

[10] C. Krishnan, R. Mohayaee, E. Ó. Colgáin, M. M. Sheikh-Jabbari and L. Yin, [arXiv:2105.09790 [astro-ph.CO]].

[11] P. Fleury, H. Dupuy and J. P. Uzan, Phys. Rev. Lett. **111** (2013), 091302 [arXiv:1304.7791 [astro-ph.CO]].

[12] D. J. Schwarz, C. J. Copi, D. Huterer and G. D. Starkman, Class. Quant. Grav. **33** (2016) no.18, 184001 [arXiv:1510.07929 [astro-ph.CO]].

[13] A. de Oliveira-Costa, M. Tegmark, M. Zaldarriaga and A. Hamilton, Phys. Rev. D **69** (2004), 063516 [arXiv:astro-ph/0307282 [astro-ph]].

[14] D. J. Schwarz, G. D. Starkman, D. Huterer and C. J. Copi, Phys. Rev. Lett. **93** (2004), 221301 [arXiv:astro-ph/0403353 [astro-ph]].

[15] K. Land and J. Magueijo, Phys. Rev. D **72** (2005), 101302 [arXiv:astro-ph/0507289 [astro-ph]].

[16] J. Kim and P. Naselsky, Astrophys. J. Lett. **714** (2010), L265-L267 [arXiv:1001.4613 [astro-ph.CO]].

[17] P. Naselsky, W. Zhao, J. Kim and S. Chen, Astrophys. J. **749** (2012), 31 [arXiv:1108.4376 [astro-ph.CO]].

[18] C. Blake and J. Wall, Nature **416** (2002), 150-152 [arXiv:astro-ph/0203385 [astro-ph]].

[19] A. K. Singal, Astrophys. J. Lett. **742** (2011), L23 [arXiv:1110.6260 [astro-ph.CO]].

[20] C. Gibelyou and D. Huterer, Mon. Not. Roy. Astron. Soc. **427** (2012), 1994-2021 [arXiv:1205.6476 [astro-ph.CO]].

[21] M. Rubart and D. J. Schwarz, Astron. Astrophys. **555** (2013), A117 [arXiv:1301.5559 [astro-ph.CO]].

[22] P. Tiwari and A. Nusser, JCAP **03** (2016), 062 [arXiv:1509.02532 [astro-ph.CO]].

[23] J. Colin, R. Mohayaee, M. Rameez and S. Sarkar, Mon. Not. Roy. Astron. Soc. **471** (2017) no.1, 1045-1055 [arXiv:1703.09376 [astro-ph.CO]].

[24] C. A. P. Bengaly, R. Maartens and M. G. Santos, JCAP **04** (2018), 031 [arXiv:1710.08804 [astro-ph.CO]].

[25] T. M. Siewert, M. Schmidt-Rubart and D. J. Schwarz, [arXiv:2010.08366 [astro-ph.CO]].

[26] N. J. Secrest, S. von Hausegger, M. Rameez, R. Mohayaee, S. Sarkar and J. Colin, Astrophys. J. Lett. **908** (2021) no.2, L51 [arXiv:2009.14826 [astro-ph.CO]].

[27] A. K. Singal, [arXiv:2106.11968 [astro-ph.CO]].

[28] A. K. Singal, [arXiv:2107.09390 [astro-ph.CO]].

[29] S. Saha, S. Shaikh, S. Mukherjee, T. Souradeep and B. D. Wandelt, [arXiv:2106.07666 [astro-ph.CO]].

[30] J. K. Webb, J. A. King, M. T. Murphy, V. V. Flambaum, R. F. Carswell and M. B. Bainbridge, Phys. Rev. Lett. **107** (2011), 191101 [arXiv:1008.3907 [astro-ph.CO]].

[31] J. A. King, J. K. Webb, M. T. Murphy, V. V. Flambaum, R. F. Carswell, M. B. Bainbridge, M. R. Wilczynska and F. E. Koch, Mon. Not. Roy. Astron. Soc. **422** (2012), 3370-3413 [arXiv:1202.4758 [astro-ph.CO]].

[32] D. Hutsemekers and H. Lamy, Astron. Astrophys. **367** (2001), 381-387 [arXiv:astro-ph/0012182 [astro-ph]].

[33] D. Hutsemekers, R. Cabanac, H. Lamy and D. Sluse, Astron. Astrophys. **441** (2005), 915-930 [arXiv:astro-ph/0507274 [astro-ph]].

[34] C. Krishnan, R. Mohayaee, E. Ó Colgáin, M. M. Sheikh-Jabbari and L. Yin, [arXiv:2106.02532 [astro-ph.CO]].

[35] K. Migkas, G. Schellenberger, T. H. Reiprich, F. Pacaud, M. E. Ramos-Ceja and L. Lovisari, Astron. Astrophys. **636** (2020), A15 [arXiv:2004.03305 [astro-ph.CO]].

[36] K. Migkas, F. Pacaud, G. Schellenberger, J. Erler, N. T. Nguyen-Dang, T. H. Reiprich, M. E. Ramos-Ceja and L. Lovisari, Astron. Astrophys. **649** (2021), A151 [arXiv:2103.13904 [astro-ph.CO]].

[37] B. E. Schaefer, Astrophys. J. **660** (2007), 16.

[38] F. Y. Wang, Z. G. Dai, and Z.-H. Zhu, Astrophys. J. **667** (2007), 1-10.

[39] L. Amati, C. Guidorzi, F. Frontera, M. Della Valle, F. Finelli, R. Landi and E. Montanari, Mon. Not. Roy. Astron. Soc. **391** (2008), 577-584 [arXiv:0805.0377 [astro-ph]].

[40] S. Capozziello, and L. Izzo. Astronom. Astrophys. **490** (2008), 31-36.

[41] M. G. Dainotti, V. F. Cardone, and S. Capozziello. Mon. Not. Roy. Astron. Soc. **391** (2008), L79–L83.

[42] L. Izzo, S. Capozziello, G. Covone, and M. Capaccioli. Astronom. Astrophys. **508** (2009), 63–67.

[43] L. Amati and M. Della Valle, International Journal of Modern Physics D **22** (2013), 1330028.

[44] J.-J. Wei, X.-F. Wu, F. Melia, D.-M. Wei, and L.-L. Feng Mon. Not. Roy. Astron. Soc. **439** (2014), 3329-3341.

[45] L. Izzo, M. Muccino, E. Zaninoni, L. Amati, and M. Della Valle. Astronom. Astrophys. **582** (2015), A115.

[46] C.-H. Tang, Y.-F. Huang, J.-J. Geng, and Z.-B. Zhang. Astrophys. J. Suppl. **245** (2019), 1.

[47] G. Risaliti and E. Lusso, Astrophys. J. **815** (2015), 33 [arXiv:1505.07118 [astro-ph.CO]].

[48] D. Zhao and J. Q. Xia, Eur. Phys. J. C **81** (2021) no.8, 694

[49] K. C. Wong, S. H. Suyu, G. C. F. Chen, C. E. Rusu, M. Millon, D. Sluse, V. Bonvin, C. D. Fassnacht, S. Taubenberger and M. W. Auger, *et al.* Mon. Not. Roy. Astron. Soc. **498** (2020) no.1, 1420-1439 [arXiv:1907.04869 [astro-ph.CO]].

[50] M. Millon, A. Galan, F. Courbin, T. Treu, S. H. Suyu, X. Ding, S. Birrer, G. C. F. Chen, A. J. Shajib and D. Sluse, *et al.* Astron. Astrophys. **639** (2020), A101 [arXiv:1912.08027 [astro-ph.CO]].

[51] S. H. Suyu, S. Huber, R. Cañameras, M. Kromer, S. Schuldt, S. Taubenberger, A. Yıldırım, V. Bonvin, J. H. H. Chan and F. Courbin, *et al.* Astron. Astrophys. **644** (2020), A162 [arXiv:2002.08378 [astro-ph.CO]].

[52] D. Watson, K. D. Denney, M. Vestergaard and T. M. Davis, Astrophys. J. Lett. **740** (2011), L49 [arXiv:1109.4632 [astro-ph.CO]].

[53] J. M. Wang, P. Du, D. Valls-Gabaud, C. Hu and H. Netzer, Phys. Rev. Lett. **110** (2013) no.8, 081301 [arXiv:1301.4225 [astro-ph.CO]]. Copy to ClipboardDownload

[54] F. La Franca, S. Bianchi, G. Ponti, E. Branchini and G. Matt, Astrophys. J. Lett. **787** (2014), L12 [arXiv:1404.2607 [astro-ph.CO]].

[55] H. Tananbaum, Y. Avni, G. Branduardi *et al.* Astrophys. J. **234** (1979) L9

[56] C. Vignali, W. N. Brandt and D. P. Schneider, Astron. J. **125** (2003), 433 [arXiv:astro-ph/0211125 [astro-ph]].

[57] D. W. Just, W. N. Brandt, O. Shemmer, A. T. Steffen,

D. P. Schneider, G. Chartas and G. P. Garmire, Astrophys. J. **665** (2007), 1004-1022 [arXiv:0705.3059 [astro-ph]].

[58] E. Lusso, A. Comastri, C. Vignali, G. Zamorani, M. Brusa, R. Gilli, K. Iwasawa, M. Salvato, F. Civano and M. Elvis, *et al.* Astron. Astrophys. **512** (2010), A34 [arXiv:0912.4166 [astro-ph.CO]].

[59] F. Salvestrini, G. Risaliti, S. Bisogni, E. Lusso and C. Vignali, Astron. Astrophys. **631** (2019), A120 [arXiv:1909.12309 [astro-ph.GA]].

[60] G. Risaliti and E. Lusso, Nature Astron. **3** (2019) no.3, 272-277 [arXiv:1811.02590 [astro-ph.CO]].

[61] E. Lusso, E. Piedipalumbo, G. Risaliti, M. Paolillo, S. Bisogni, E. Nardini and L. Amati, Astron. Astrophys. **628** (2019), L4 [arXiv:1907.07692 [astro-ph.CO]].

[62] E. Lusso, G. Risaliti, E. Nardini, G. Bargiacchi, M. Benetti, S. Bisogni, S. Capozziello, F. Civano, L. Eggleston and M. Elvis, *et al.* Astron. Astrophys. **642** (2020), A150 [arXiv:2008.08586 [astro-ph.GA]].

[63] M. M. Phillips, Astrophys. J. Lett. **413** (1993), L105-L108

[64] T. Yang, A. Banerjee and E. Ó Colgáin, Phys. Rev. D **102** (2020) no.12, 123532 [arXiv:1911.01681 [astro-ph.CO]].

[65] H. Velten and S. Gomes, Phys. Rev. D **101** (2020) no.4, 043502 [arXiv:1911.11848 [astro-ph.CO]].

[66] N. Khadka and B. Ratra, Mon. Not. Roy. Astron. Soc. **492** (2020) no.3, 4456-4468 [arXiv:1909.01400 [astro-ph.CO]].

[67] N. Khadka and B. Ratra, Mon. Not. Roy. Astron. Soc. **497** (2020) no.1, 263-278 [arXiv:2004.09979 [astro-ph.CO]].

[68] A. Banerjee, E. Ó Colgáin, M. Sasaki, M. M. Sheikh-Jabbari and T. Yang, Phys. Lett. B **818** (2021), 136366 [arXiv:2009.04109 [astro-ph.CO]].

[69] T. Delubac *et al.* [BOSS], Astron. Astrophys. **574** (2015), A59 [arXiv:1404.1801 [astro-ph.CO]].

[70] T. M. C. Abbott *et al.* [DES], [arXiv:2107.04646 [astro-ph.CO]].

[71] H. du Mas des Bourboux, J. Rich, A. Font-Ribera, V. de Sainte Agathe, J. Farr, T. Etourneau, J. M. Le Goff, A. Cuceu, C. Balland and J. E. Bautista, *et al.* Astrophys. J. **901** (2020) no.2, 153 [arXiv:2007.08995 [astro-ph.CO]].

[72] N. Khadka and B. Ratra, Mon. Not. Roy. Astron. Soc. **502** (2021) no.4, 6140-6156 [arXiv:2012.09291 [astro-ph.CO]].

[73] N. Khadka and B. Ratra, [arXiv:2107.07600 [astro-ph.CO]].

[74] E. Ó. Colgáin and M. M. Sheikh-Jabbari, Class. Quant. Grav. **38** (2021) no.17, 177001 [arXiv:2102.09816 [gr-qc]].

[75] N. Khadka, O. Luongo, M. Muccino and B. Ratra, [arXiv:2105.12692 [astro-ph.CO]].

[76] M. Demianski, E. Piedipalumbo, D. Sawant and L. Amati, Astron. Astrophys. **598** (2017), A112 [arXiv:1610.00854 [astro-ph.CO]].

[77] D. Camarena and V. Marra, Mon. Not. Roy. Astron. Soc. **504** (2021), 5164-5171 [arXiv:2101.08641 [astro-ph.CO]].

[78] G. Efstathiou, Mon. Not. Roy. Astron. Soc. **505** (2021) no.3, 3866-3872 [arXiv:2103.08723 [astro-ph.CO]].

[79] F. Melia, Mon. Not. Roy. Astron. Soc. **489** (2019) no.1, 517-523 [arXiv:1907.13127 [astro-ph.CO]].

[80] M. Demianski, E. Piedipalumbo, D. Sawant and L. Amati, Mon. Not. Roy. Astron. Soc. **506** (2021) no.1, 903-918 [arXiv:1911.08228 [astro-ph.CO]].

[81] H. Khoraminezhad, M. Viel, C. Baccigalupi and M. Archidiacono, JCAP **07** (2020), 039 [arXiv:2001.10252 [astro-ph.CO]].

[82] M. Lindner, K. Max, M. Platscher and J. Rezacek, JCAP **10** (2020), 040 [arXiv:2002.01487 [astro-ph.CO]].

[83] X. Zheng, K. Liao, M. Biesiada, S. Cao, T. H. Liu and Z. H. Zhu, [arXiv:2002.09909 [astro-ph.CO]].

[84] A. Mehrabi and S. Basilakos, Eur. Phys. J. C **80** (2020) no.7, 632 [arXiv:2002.12577 [astro-ph.CO]].

[85] T. Liu, S. Cao, J. Zhang, M. Biesiada, Y. Liu and Y. Lian, [arXiv:2005.13990 [astro-ph.CO]].

[86] M. Demianski, E. Lusso, M. Paolillo, E. Piedipalumbo and G. Risaliti, Front. Astron. Space Sci. **7** (2020), 69 [arXiv:2010.05289 [astro-ph.CO]].

[87] J. P. Hu, Y. Y. Wang and F. Y. Wang, Astron. Astrophys. **643** (2020), A93 [arXiv:2008.12439 [astro-ph.CO]].

[88] O. Luongo and M. Muccino, Astron. Astrophys. **641** (2020), A174 [arXiv:2010.05218 [astro-ph.CO]].

[89] S. Cao, J. Ryan, N. Khadka and B. Ratra, Mon. Not. Roy. Astron. Soc. **501** (2021) no.1, 1520-1538 [arXiv:2009.12953 [astro-ph.CO]].

[90] L. Speri, N. Tamanini, R. R. Caldwell, J. R. Gair and B. Wang, Phys. Rev. D **103** (2021) no.8, 083526 [arXiv:2010.09049 [astro-ph.CO]].

[91] O. Luongo and M. Muccino, Mon. Not. Roy. Astron. Soc. **503** (2021) no.3, 4581-4600 [arXiv:2011.13590 [astro-ph.CO]].

[92] M. Muccino, L. Izzo, O. Luongo, K. Boshkayev, L. Amati, M. Della Valle, G. B. Pisani and E. Zaninoni, Astrophys. J. **908** (2021) no.2, 181 [arXiv:2012.03392 [astro-ph.CO]].

[93] X. Li, R. E. Keeley, A. Shafieloo, X. Zheng, S. Cao, M. Biesiada and Z. H. Zhu, [arXiv:2103.16032 [astro-ph.CO]].

[94] Y. Lian, S. Cao, M. Biesiada, Y. Chen, Y. Zhang and W. Guo, Mon. Not. Roy. Astron. Soc. **505** (2021) no.2, 2111-2123 [arXiv:2105.04992 [astro-ph.CO]].

[95] F. Y. Wang, J. P. Hu, G. Q. Zhang and Z. G. Dai, [arXiv:2106.14155 [astro-ph.HE]].

[96] A. R. King and G. F. R. Ellis, Commun. Math. Phys. **31** (1973), 209-242

[97] G. F. R. Ellis and H. van Elst, NATO Sci. Ser. C **541** (1999), 1-116 [arXiv:gr-qc/9812046 [gr-qc]].

[98] A. Lewis, [arXiv:1910.13970 [astro-ph.IM]].